JOURNAL OF AIRCRAFT
Vol. 41, No. 2, March–April 2004

Attachment-Line Approach for Design of a Wing-Body Leading-Edge Fairing

Bas W. van Oudheusden,* Caspar B. Steenaert,† and Loek M. M. Boermans‡
Delft University of Technology, 2600 GB Delft, The Netherlands

A simplified procedure is presented for the design of a leading-edge fairing of a wing-body combination. The design aims at optimizing the design of the fairing, which is to serve the double purpose of eliminating separation near the wing-body junction, as well as minimizing leading-edge contamination of the laminar wing. The design optimization procedure is based on the analysis of the viscous-flow performance of a fairing of prescribed geometry. First, a panel method is used to determine the inviscid flow around the fairing. This is then followed by an integral-method calculation of the boundary-layer development on the attachment line along the body and the fairing. As an application, a fairing was designed for a straight NACA0015 wing mounted on a flat plate. Tests in the wind tunnel confirmed the effectiveness of the fairing.

Nomenclature

A, B	=	fairing dimensions
C_E	=	entrainment coefficient
C_f	=	normalized skin-friction coefficient, $\tau_{\text{wall}}/\frac{1}{2}\rho U_\infty^2$
c	=	wing chord
c_f	=	skin-friction coefficient, $\tau_{\text{wall}}/\frac{1}{2}\rho U_e^2$
H, H_1	=	boundary-layer shape factors
Re	=	Reynolds number
r	=	crossflow model switching parameter
U_e, W_e	=	external flow velocity components
U_∞	=	freestream velocity
u, v, w	=	velocity components
x, y, z	=	Cartesian coordinates
δ	=	boundary-layer thickness
δ^*	=	displacement thickness
θ	=	momentum thickness
μ, μ_T	=	dynamic viscosity; turbulent viscosity
ν	=	kinematic viscosity, μ/ρ
ρ	=	density
τ	=	shear stress

Introduction

Background

MODERN high-performance sailplanes are designed to operate at the top of aerodynamic efficiency, with an optimized fuselage design and wings with extensive regions of laminar flow. In this context the wing-body integration remains an aspect of the utmost concern.[1,2] Simply attaching the straight wing to the fuselage (compare the geometry of Fig. 1) will cause a large region of detached flow near the junction, where the fuselage boundary layer encounters the strong pressure rise of the wing stagnation region. This flow behavior is usually referred to as "separation" and takes the form of a horseshoe vortex, which wraps itself around the root of the wing.[3] The common measure to control this separation is by applying a fairing that modifies the shape of the junction.[4,5] For influencing the vortex formation the leading-edge shape of the junction is of primary importance, although additional care has to be taken in the further shaping of the wing root region in order to prevent separation further downstream. In the present application range there is a second consideration in the design of the fairing, namely, that of the contamination of the laminar wing by the turbulent boundary layer on the fuselage.[2] Fairing design has in that case to serve a twofold purpose, of eliminating separation as well as promoting a rapid relaminarization of the boundary-layer flow. Evidently, similar considerations also apply when pursuing laminar flow technology on larger aircraft, such as in the recent European ELFIN project.

The complex flow structure that occurs near a wing-body junction has been the subject of intensive study. Recent reviews have been given by Simpson[3,6] and Arnott.[7] Fundamental experimental studies on the junction flow of idealized wing-plate junctions, including the effect of leading-edge fairings, have been performed, notably at NASA Langley Research Center,[8–10] Virginia Polytechnic Institute and State University,[11–14] and the University of London, Queen Mary and Westfield College.[15] Some attention might be required with respect to the proper topology of the junction flow, in particular regarding the definition of flow separation. Observation of mean flow visualizations reveals the appearance of a convergence line in the streakline pattern on the plate in front of the obstacle. This creates a saddle-point singularity on the attachment line, which reflects that flow reversal occurs in the symmetry plane. Traditionally, this singularity has been interpreted as a proper separation point, in the sense that in the symmetry plane the flow leaves the surface (i.e., the streamline pattern displays a half-saddle structure) and flows into the vortex. However, a number of careful studies[16,17] have revealed that an alternative flow topology exists, where the streamline pattern in the symmetry plane near the singularity is that of an inflowing seminode. This peculiar structure of the separation point is only possible in three-dimensional flow with lateral outflow. In this configuration the vortex is fed only by the upper part of the boundary layer, while the lower part adjacent to the wall flows downward as it is deflected out of the symmetry plane. It remains unclear if this structure persists at high Reynolds number and/or in turbulent flow or that the traditional structure prevails then. In addition, Hung et al.[17] observed that the simplest flow structure is one where the inflowing seminode occurred without vortex, revealing that flow reversal near the plate is not necessarily accompanied by the formation of a horseshoe vortex. Strictly speaking, the nature of the point where the skin friction first vanishes and flow reversal occurs should be interpreted under these conditions as an attachment point rather than a separation point. However, for reasons of convention and convenience we would like to continue referring to the appearance of flow reversal in the symmetry plane as separation, but bearing in mind the possible alternative topology of the streamlines near the flow-reversal point.

Received 12 December 2002; revision received 3 June 2003; accepted for publication 6 June 2003.

*Associate Professor, Faculty of Aerospace Engineering; B.W.vanOudheusden@lr.tudelft.nl.
†Graduate Student, Faculty of Aerospace Engineering.
‡Associate Professor, Faculty of Aerospace Engineering.

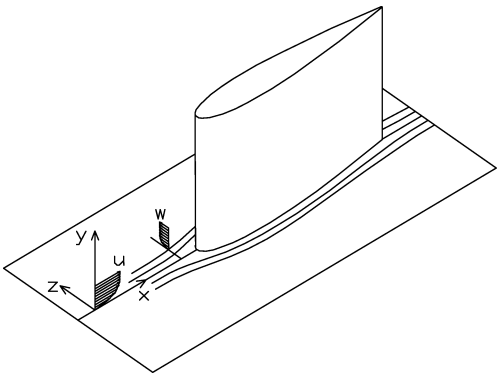

Fig. 1 Basic geometry of the wing-body junction and coordinate system.

Because of the complex flow structure that occurs near the wing-body junction, the determination of the fairing shape has traditionally been a design art, relying heavily on craftsmanship, and where the fairing optimization is usually obtained in an empirical process of (experimental) trial and error (for example, see Ref. 18). A numerical simulation of the junction flow to assist the design faces the challenges of capturing a highly three-dimensional viscous and usually turbulent flow.[19,20] Green and Whitesides recently proposed a fairing design method based on Navier–Stokes computations.[21] Evidently, the amount of computing effort required for such an approach is very large, which makes it too demanding for many routine design applications. Also, flow relaminarization is not yet within the capabilities of standard computational fluid dynamics (CFD). Therefore, in many low-speed aircraft designs the common approach is still to use panel methods to determine the inviscid flow, in combination with simplified boundary-layer methods to assess the viscous flow performance.[1,2] Also in this line Maughmer et al.[1] suggested the assessment of wing-integration geometries by applying integral boundary-layer methods along streamlines.

Preliminary Design Considerations

In this study a simplified design procedure is proposed, which in its present form is applied to symmetrical flow situations. The study considers a symmetrical wing under zero angle of attack, while the fuselage is modelled as a flat plate. The incoming boundary layer on the plate is taken to be turbulent as is the case in real applications. Furthermore, the flow is considered incompressible.

The flow analysis is based on a classical boundary-layer approach in which first the inviscid flow for a proposed fairing geometry is determined with a panel method. The relevant properties of the inviscid pressure distribution are then supplied to a boundary-layer computation to assess the viscous-flow performance of the fairing. Although this approach would evidently be incorrect for flows with large separation, as in the case of the junction without fairing, the design aim is a fairing without separation, for which there is a reasonable justification of this approach.

A second important simplifying aspect of the procedure is that the boundary-layer development is computed only on the attachment line, which is the dividing streamline along the plate and the fairing and wing leading edges. It is assumed that this is sufficiently representative of the performance of the fairing as a whole. It is likely that the steepest adverse pressure gradient will occur along the attachment line and that as a result the most upstream location of flow reversal is to be found on this line. Separation has to be prevented by a correct design of a fairing, and it would seem that preventing flow reversal on the attachment line is a necessary and possibly sufficient condition.

These computational tools are then applied to study the effect of altering the shape and dimensions of the fairing and, thus, to optimize it in terms of the design requirements.

Flow Analysis

The flow-analysis procedure that is applied in the present study is based on a classical boundary-layer approach and exploits the basic simplifications that apply in a symmetrical flow situation. The flow in the symmetry plane can be determined without the need of considering the spanwise dimension.[22] A quasi-two-dimensional boundary-layer computation along the attachment line then suffices, for which standard two-dimensional methods need to be extended to take the lateral flow-relieving effect into account.[23–25] In the present study Head's turbulent integral entrainment method was used.[26] The computation yields the development of the boundary-layer shape factor and momentum thickness, which are used to assess flow reversal (separation) and relaminarization by semi-empirical criteria.

The basic coordinate system is taken as shown in Fig. 1, where initially on the plate the x axis is in the direction of the freestream, the y axis is normal to the plate, and z axis is in the lateral direction along the plate and normal to the symmetry plane of the configuration. The viscous flow equations governing the boundary-layer development are given with respect to a body-fitted, locally orthonormal coordinate system: x follows the flow along the surface in the symmetry plane, y is normal to the local surface, and z is in the lateral direction, normal to both x and y. The corresponding velocity components are u, v, and w. The logical extension of this coordinate system onto the wing implies that x runs in the spanwise direction along the leading edge of the wing and z in the chordwise direction. It can be noted here that the consequence of this is that on the wing the notation is the reverse of that commonly used for swept-wing flow analysis.

Boundary-Layer Development in Plane of Symmetry

For reasons of symmetry, the lateral velocity component w is zero at the symmetry plane and must be replaced by its lateral gradient $\tilde{w} = \partial w/\partial z$ as primary variable. The governing equations in the symmetry plane ($z = 0$) are then given by the continuity equation, the x-momentum equation, and the z derivative of the z-momentum equation[22]:

$$\frac{\partial u}{\partial x} + \frac{\partial v}{\partial y} + \tilde{w} = 0 \tag{1}$$

$$u\frac{\partial u}{\partial x} + v\frac{\partial u}{\partial y} = U_e\frac{dU_e}{dx} + \frac{1}{\rho}\frac{\partial \tau_x}{\partial y} \tag{2}$$

$$u\frac{\partial \tilde{w}}{\partial x} + v\frac{\partial \tilde{w}}{\partial y} + \tilde{w}^2 = U_e\frac{d\tilde{W}_e}{dx} + \tilde{W}_e^2 + \frac{1}{\rho}\frac{\partial \tilde{\tau}_z}{\partial y} \tag{3}$$

where τ_x is the (total) shear stress in the x direction and $\tilde{\tau}_z = \partial \tau_z/\partial z$ the lateral gradient of the shear stress in the z direction. To illustrate the character of the shear-stress terms, let us consider for convenience an eddy-viscosity model for the turbulent contribution to the shear stresses:

$$\tau_x = (\mu + \mu_T)\frac{\partial u}{\partial y}, \qquad \tilde{\tau}_z = (\mu + \mu_T)\frac{\partial \tilde{w}}{\partial y} \tag{4}$$

With the mean flow being planar in the symmetry plane, symmetry arguments show that any rational extension of a two-dimensional turbulence model to three-dimensional flow will again reduce to the original two-dimensional model at the symmetry plane itself. For example, approaching the turbulent viscosity according to a mixing-length concept will give

$$\mu_T = \rho\ell^2\frac{\partial u}{\partial y} \tag{5}$$

with the mixing length $\ell = \ell(y)$ a function of y only; hence, the turbulent viscosity becomes a function of y alone, too. The preceding considerations are presented here only as an argument to show that for the turbulence modeling in the symmetry plane two-dimensional flow models can be used with reasonable confidence.

It might now be obvious that Eqs. (1–3) allow the calculation of the boundary-layer development in the symmetry plane alone, as the lateral spatial dimension z is absent in them. It can be noted that the streamwise-momentum equation (2) has the same form as for two-dimensional flow. As matching conditions with the inviscid freestream, the values of U_e and $\tilde{W}_e$ are required as function of

x. These are to follow from an inviscid flow calculation for the complete wing-plate-fairing combination.

Some Basic Characteristics of Junction Flow

Some typical aspects of the junction flow structure are highlighted here to illustrate how the fairing can be seen to function in eliminating the flow separation at the wing junction and how the inviscid (external) flow conditions are involved in this process.

In the absence of a fairing (as in Fig. 1), the geometrical discontinuity at the leading edge of the junction creates a stagnation point in the inviscid flow. As a result of this pressure rise, the viscous flow will display flow reversal and separation. Note that for the geometry of a straight wing without fairing, the inviscid flow would be invariant with y. As a direct consequence of the continuity equation, we then find that along the plate the following relation holds:

$$\tilde{W}_e = -\frac{\mathrm{d}U_e}{\mathrm{d}x} \tag{6}$$

This shows, with $\mathrm{d}U_e/\mathrm{d}x < 0$ when approaching the stagnation point of the three-dimensional configuration, that $\tilde{W}_e > 0$, resulting in a lateral outflow out of the symmetry plane, which is an illustration of the well-known three-dimensional flow-relieving effect. Although this effect will reduce the boundary-layer growth and delay flow reversal in comparison to a two-dimensional flow that is subjected to the same streamwise pressure gradient, this effect is clearly insufficient to prevent separation. Massive separation occurs, giving rise to a complex separated flowfield.[3]

On the wing at a large distance from the plate, on the other hand, the inviscid flow will resemble that around an infinite wing, which will be quantified later.

The function of the fairing can now be seen in the preceding perspective, in that it removes the stagnation point and provides a smooth and gradual transition from the conditions on the flat plate to the more-or-less constant conditions along the wing. First, the fairing reduces the severity of the adverse pressure gradient, and second, it gives the flow-relieving effect sufficient opportunity to prevent flow reversal altogether. It might be obvious that increasing the size of the fairing will progressively facilitate this process. However, with the viscous flow, that is, the fuselage boundary layer, now extending onto the wing, it is evident that any flow turbulence on the plate will be transported onto the wing as well. But the local Reynolds number of the viscous flow will decline rapidly as both the edge velocity and the boundary-layer thickness decrease, and it will ultimately become so low that the turbulence decays completely and laminarization of the flow occurs.[27,28] It can be understood that the second design requirement, which is that minimal contamination of the (laminar) wing requires a rapid laminarization, is served by reducing the size of the fairing. A further reason to limit the size of the fairing is to reduce the increase in wetted area and the associated friction drag.

The boundary-layer computation is now to function as a quantitative tool to assess both these aspects, that is, preventing separation and promoting laminarization of the viscous flow on the fairing.

Integral Boundary-Layer Equations

For the boundary-layer calculation an integral approach is used, for which Head's entrainment method[26] was adapted to take the extra flow-relieving effect into account. The basic equations used are the streamwise momentum equation and the entrainment equation, supplemented by the usual closure relations.

The integral streamwise momentum equation is obtained by integrating Eq. (2) over the boundary-layer thickness, yielding

$$\frac{\mathrm{d}\theta}{\mathrm{d}x} = \frac{c_f}{2} - (2+H)\frac{\theta}{U_e}\frac{\mathrm{d}U_e}{\mathrm{d}x} - \frac{\tilde{W}_e}{U_e}\int_0^\delta \frac{\tilde{w}}{\tilde{W}_e}\left(1-\frac{u}{U_e}\right)\mathrm{d}y \tag{7}$$

The last term on the right-hand side disappears when $\tilde{w}=0$, which reduces the equation to the well-known Karman momentum integral for two-dimensional flow.[29]

The entrainment equation describes the rate at which the boundary-layer turbulence spreads into the neighboring outer flow and is essentially the continuity equation integrated over the boundary-layer thickness δ, yielding:

$$\frac{1}{U_e}\frac{\mathrm{d}}{\mathrm{d}x}(U_e\theta H_1) = C_E - \frac{\tilde{W}_e}{U_e}\int_0^\delta \frac{\tilde{w}}{\tilde{W}_e}\,\mathrm{d}y \tag{8}$$

where $H_1 = (\delta - \delta^*)/\theta$ and $C_E = V_E/U_e$ with V_E the entrainment velocity, that is, the velocity rate at which fluid entrains across the edge of the boundary layer:

$$V_E = U_e\frac{\mathrm{d}\delta}{\mathrm{d}x} - v_\delta \tag{9}$$

As the flow in the symmetry plane is planar, we assume that closure relations for two-dimensional flow can be applied. The following correlations are used for the entrainment coefficient C_E and the shape factor H_1:

$$C_E = F(H_1) = 0.0306(H_1-3)^{-0.653}$$
$$H_1 = 1.535(H-0.7)^{-2.715} + 3.3 \tag{10}$$

together with White's skin-friction law[29]:

$$c_f \approx \frac{0.3e^{-1.33H}}{(\log_{10} Re_\theta)^{1.74+0.31H}} \tag{11}$$

Modeling of Crossflow Terms

Equations (7), (8), (10), and (11) form a closed system with which the boundary development can be calculated, provided that the crossflow terms in Eqs. (7) and (8) are modeled. These express the integrated lateral flow-relieving effect, in terms of a lateral transport of momentum-deficit in Eq. (7) and of mass in the boundary layer in Eq. (8). Both terms are seen to reduce the boundary-layer growth when $\tilde{w} > 0$ (lateral outflow). One option to model these terms would be to determine the crossflow from an additional equation, typically the integral form of the lateral momentum equation, Eq. (3). Such an approach is common to general three-dimensional integral methods and was also applied by Cumpsty and Head,[23–25] who then proceeded by representing the crossflow by a single parameter (typically, the crossflow angle at the wall), the value of which can then be obtained from this third equation.

In the present analysis, however, we propose an even simpler approach to the crossflow term, relying on the typical flow configurations that occur in the present application. Typically, the streamwise velocity profile develops in an adverse pressure gradient, whereas in the lateral direction the flow is accelerated from the symmetry plane outwards. Therefore, we can assume the w profile to be fuller than the u profile:

$$u/U_e \le \tilde{w}/\tilde{W}_e \le 1 \tag{12}$$

This can be generalized by proposing

$$\tilde{w}/\tilde{W}_e = r + (1-r)(u/U_e) \qquad 0 \le r \le 1 \tag{13}$$

which introduces the switching function r for notational convenience. We can now proceed by considering either of the two limiting assumptions:

Assumption 1:

$$\tilde{w}/\tilde{W}_e \approx u/U_e \qquad (r=0) \tag{14a}$$

Assumption 2:

$$\tilde{w}/\tilde{W}_e \approx 1 \qquad (r=1) \tag{14b}$$

It is clear that in the conditions considered, assumption 1 will be a conservative estimate that underpredicts the lateral flow relieving, whereas, on the other hand, assumption 2 might be too optimistic in that it overestimates this effect. If both assumptions are considered separately, the outcome is expected to give the typical range for the boundary-layer properties, like the shape factor and the momentum loss thickness, and the correct solution is likely to be somewhere

in between. Far upstream of the wing, the shape of both velocity profiles is probably comparable, so that the first equality holds. (It can be shown that this is exact for the laminar boundary layer at the leading edge of the plate, where both u and w display Blasius profiles). This is of limited relevance, though, as the crossflow is still small in magnitude there. Once the crossflow effect becomes important, that is, when approaching the fairing, the adverse pressure gradient will have become appreciable as well, and under this condition the second equality is likely a better approximation.

The adoption of either of these assumptions allows the integrals in Eqs. (7) and (8) to be expressed in terms of the streamwise velocity profile:

$$\frac{\mathrm{d}\theta}{\mathrm{d}x} = \frac{c_f}{2} - (2+H)\frac{\theta}{U_e}\frac{\mathrm{d}U_e}{\mathrm{d}x} - \frac{\tilde{W}_e}{U_e}(rH+1-r)\theta \qquad (15)$$

$$\frac{1}{U_e}\frac{\mathrm{d}}{\mathrm{d}x}(U_e\theta H_1) = F(H_1) - \frac{\tilde{W}_e}{U_e}(rH+H_1)\theta \qquad (16)$$

The equations can now be solved in combination with the closure relations (10) and (11).

Swept-Wing Attachment Line

The boundary layer of the leading edge of a swept wing is considered here as an interesting test case for assessing the suggested approach to model the flow-relieving crossflow effect in the boundary-layer calculation. For an infinite wing the flow near the attachment line is especially simple, as it is invariant along the spanwise direction and characterized by only a single dimensionless parameter, which is the Reynolds number. This flow is in itself attractive as an elementary and well-documented problem,[25,30–32] which is dominated by the flow-relieving effect. On the other hand, the attachment-line boundary layer has an evident technological relevance, in particular in the context of the leading-edge contamination on swept-wing aircraft. For this reason it has received wide attention, especially with regard to the stability of the laminar flow and the possibility to suppress or eliminate the effect of turbulence at the wing root that originates from the fuselage boundary layer.[33] This latter aspect of the swept-wing boundary layer is similar to what is happening on the fairing, and related experimental and numerical evidence will be used in a subsequent section to define a laminarization criterion for the fairing boundary layer.

The single nondimensional parameter that characterizes the viscous flow near the attachment line under incompressible conditions is the Reynolds number, defined as

$$Re = U_e \Big/ \sqrt{\nu \tilde{W}_e} \qquad (17)$$

Here, U_e and $\tilde{W}_e$ are the spanwise component and the chordwise gradient of the freestream velocity, respectively. Both are constant in case of an infinite swept wing and relate to the freestream velocity and the wing properties by

$$U_e = U_\infty \sin\Lambda, \qquad \tilde{W}_e = \varepsilon(U_\infty/R_0)\cos\Lambda \qquad (18)$$

with wing sweep Λ, nose radius R_0, and a geometry factor ε, where for example, $\varepsilon = (1 + t/c)$ for a wing with an elliptical cross section of maximum thickness t and chord length c. With these expressions the preceding Reynolds number can be written as

$$Re = \sqrt{\frac{U_\infty R_0}{\nu}}\frac{\sin\Lambda}{\sqrt{\varepsilon\cos\Lambda}} \qquad (19)$$

The Reynolds number is seen to increase with freestream speed, nose radius, and sweep angle.

Effect of Reynolds Number

For both laminar and turbulent flow the boundary-layer properties remain constant along the span of the swept wing, as the boundary-layer growth by viscous diffusion and turbulent entrainment is balanced by the depletion of the boundary-layer flow through the lateral flow relieving.

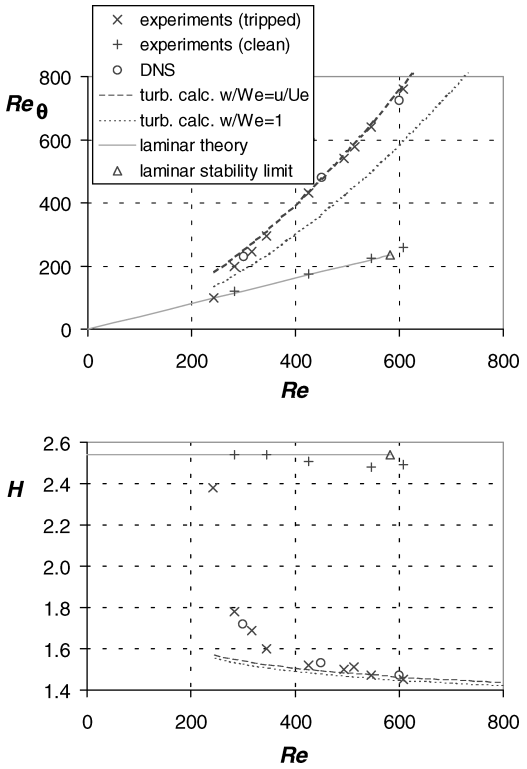

Fig. 2 Results for the attachment-line boundary layer of an infinite-swept wing (experimental data from Ref. 25; DNS data from Ref. 32).

The laminar flow solution has been documented, for example by Crabtree et al.[34] The spanwise velocity profile displays a shape factor of $H = 2.54$, which is comparable to that of the Blasius boundary layer ($H = 2.59$), whereas the momentum thickness Reynolds number is given by

$$Re_\theta = U_e\theta/\nu = 0.405Re \qquad (20)$$

Whether the fully developed flow situation is laminar or turbulent depends on the value of the Reynolds number and, for a certain intermediate range of Reynolds number, also on the initial disturbance level, as shown by measurements[25] and Direct Numerical Simulation (DNS) simulations[32] (see also Fig. 2). For small initial disturbances the flow is observed to remain laminar for Reynolds numbers up to about 600, whereas Poll[31] reports an upper value of 570 for this. These values compare well with predictions from linear stability theory,[35] which yield a critical value of $Re = 583$. In the presence of large disturbances, the flow is found to return to a laminar state when $Re < 250$ and to show intermittent turbulence for Re between 250 and 400.

The theoretical stability point as well as the experimentally observed relaminarization point were confirmed by Spalart's DNS results.[32] Using Eq. (20), the corresponding values for Re_θ are 235 for laminar instability and about 100 for relaminarization.

Prediction of Boundary-Layer Properties

By introducing the x invariance of the infinite-wing flow into the governing Eqs. (15) and (16) and invoking Eq. (17), we obtain

$$c_f/2 = \left(Re_\theta \Big/ Re^2\right)(rH + 1 - r) \qquad (21)$$

$$F(H_1) = \left(Re_\theta \Big/ Re^2\right)(rH + H_1) \qquad (22)$$

Together with the closure relations, Eqs. (10) and (11), the boundary-layer properties can be determined as function of the reference Reynolds number. The results of the predictions for the two crossflow assumptions proposed in Eq. (14) are shown in Fig. 2.

The agreement with the experimental and DNS data is especially good for the assumption that the two flow profiles are equal, $\tilde{w}/\tilde{W}_e = u/U_e$. This observation, however, does not necessarily imply that this is also the preferred approach for the actual calculation

of the fairing boundary layer. First, there is some fortuity in the agreement of prediction and data, as the error introduced by the crossflow assumption is partially cancelled by the error in the skin friction, which is predicted too low because of the use of typical large-Reynolds-number closure relations at these rather low Reynolds numbers. Second, on the attachment line of the infinite wing the pressure gradient in the flow direction is zero, so that the streamwise velocity profile is similar to that of a flat-plate boundary layer. On the fairing, on the other hand, the pressure gradient will be adverse, causing larger differences to develop between the streamwise and lateral velocity profiles.

Relaminarization Criterion

As discussed, the turbulent fuselage boundary layer extends onto the fairing and will ultimately relaminarize. One of the purposes of the fairing design is to establish a laminar flow on the wing as close to the wing root as possible. The observations of the behavior of the swept-wing boundary layer can provide important evidence with which to quantify this relaminarization.

The stability of the attachment-line boundary layer is directly of relevance to the phenomenon of leading-edge contamination. This effect was first discovered in the 1950s when attempts to realize natural laminar flow on swept wings were found to be hindered by turbulence travelling along the leading edge. Pioneering work in this field was performed by Pfenninger,[27,36] Gaster,[30] and Poll,[31] among others. Leading-edge contamination causes the wing to become fully turbulent before the condition of linear instability of the laminar flow is reached. This premature transition is triggered by large initial disturbances, in particular the turbulence in the fuselage boundary layer at the wing root, which propagate and contaminate the attachment-line boundary layer in spanwise direction.

One of the first to investigate and report this phenomenon was Pfenninger,[36] who observed when testing the 30-deg swept X-21 wing that the flow on the inner part of the wing was turbulent over the full chord, but laminar over the full chord on the outer part of the wing. When investigating the effect of disturbances at the attachment line in more detail, a marked influence of the value of $Re_{\theta,\mathrm{al}}$, the momentum Reynolds number at the attachment line, was observed. When $Re_{\theta,\mathrm{al}}$ was smaller than 90, only a chordwise turbulent wedge developed downstream of an attachment-line roughness. Between 90 and 105, the spread became larger, and turbulent bursts developed along the attachment line. Above the value of 105, the attachment line became fully turbulent.

Under these conditions a turbulent attachment-line flow will act at every position along the leading edge as a source of turbulence, comparable to a local roughness element, which makes the flow turbulent over the full chord. As found by Pfenninger, the turbulence can only propagate in spanwise direction when Re_θ is larger than about 100. This then explains both aspects of the X-21 wing, namely, the inner wing was affected by leading-edge contamination, but as the wing was tapered the nose radius and hence the Reynolds number decrease along the span. When this value falls below the critical threshold of about 100, the leading-edge contamination is terminated. Similar values (100–110) for this phenomenon were reported by Gaster[30] and Poll,[31] and the swept-wing data discussed before.[25,32] Note that this value is comparable to the disturbance threshold for developed pipe flow (equivalent $Re_\theta \approx 88$) as quoted by Preston.[37]

The situation on the fairing is similar to that on the swept wing, and it is therefore assumed that the critical value of $Re_\theta = 100$ can be used as an indication of the location of relaminarization on the fairing as well. The exact value of this threshold might not be very critical, as Re_θ will be seen to decrease precipitously on the fairing. Also, the method is primarily used to compare the relative performance of different fairing shapes. However, there might be some concern in applying a threshold value derived under near-equilibrium conditions (on the wing), in situations where the Reynolds number changes rapidly (on the fairing). On the other hand, as observed by Spalart in his DNS simulations,[32] relaminarization can proceed rapidly once it sets in.

Fairing Design

The fairing design method was applied to a symmetrical test configuration of a straight wing with a NACA 0015 section mounted on a flat plate. The design conditions were taken to resemble a sailplane configuration (see Fig. 3) under normal flight conditions. The wing chord was chosen as 0.75 m, and starting conditions for the boundary layer were prescribed at the position 0.5 m upstream of the (original) wing leading edge.

Definition of Fairing Geometry

The fairing is formed by stretching the segment of the wing airfoil in front of the point of maximum thickness (which is at 30% chord), as indicated in Fig. 4. Linear stretching in the direction parallel to the wing chord is applied, and as the thickness distribution of the NACA 4-digit airfoil series is described analytically[38] this stretching procedure can be carried out easily and accurately. The fairing shape is defined by prescribing the leading-edge curve in the symmetry plane. In the present investigation this was taken as a quarter-ellipse that is tangent to both the plate and the wing leading edge, with length A and height B. This means that the fairing shape is then completely determined by prescribing values for A and B.

The performance of the fairing can now be analyzed in relation to the values of A and B. The two basic requirements the fairing has to fulfill are that no separation (flow reversal) takes place and that the boundary layer becomes laminar as close to the wing root as possible. For a particular fairing the inviscid flow was determined with a panel method, and boundary-layer calculations were performed for two values of the freestream velocity (20 and 50 m/s; corresponding Reynolds numbers based on wing chord are $1–2.5 \times 10^6$) and using the two different assumptions for the crossflow effect [see Eq. (14)]. In the following two sections an illustration of the calculations will be given for one particular fairing geometry.

The closeness of the viscous flow to separation is assessed on the basis of the value of the shape factor H. When using the conservative estimate of the crossflow effect, Eq. (14a), flow reversal was considered to be prevented if H did not exceed 3. For the other assumption, which overpredicts the crossflow effect, some safety margin was applied in the design in requiring that H was not to exceed a value of 2.25 on the fairing. Relaminarization was assumed to occur when Re_θ falls below 100.

The optimum fairing size was determined by a selective exploration of the (A, B) space. Varying the length A of the fairing shows that a minimum length is required to prevent separation and that the longer the fairing the lower the maximum value of H. For a given length there is a (shallow) optimum for the height B in terms of preventing separation, as interpreted from the lowest value of maximum H. In the same way the laminarization height is found to increase with both A and B.

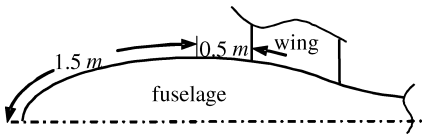

Fig. 3 Sailplane fuselage-wing geometry.

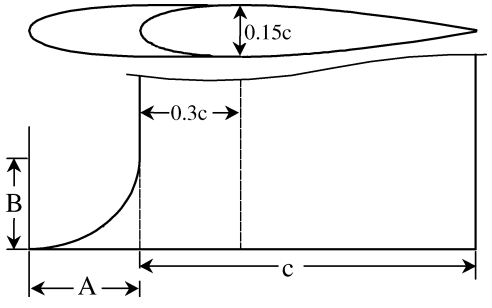

Fig. 4 Fairing geometry.

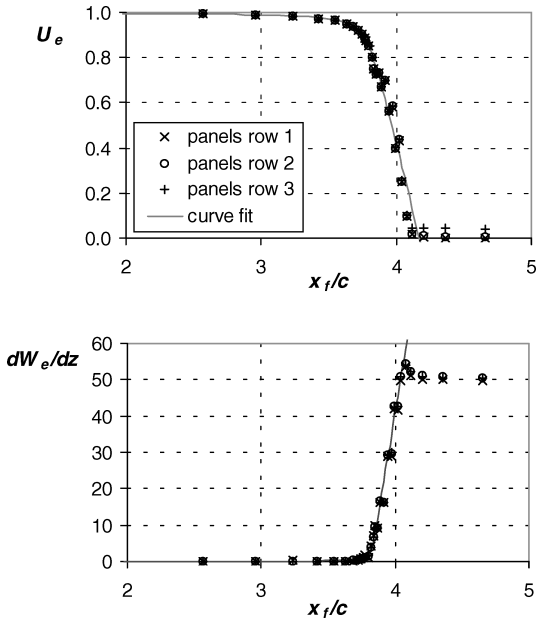

Fig. 5 Inviscid flow properties from panel calculations (large fairing, $A = 0.21c$, $B = 0.175c$).

Based on these considerations, two optimal fairing shapes were selected. With the conservative approach a fairing was designed with $A = 0.21c$ and $B = 0.175c$, whereas with the optimistic approach a smaller fairing was obtained with $A = 0.14c$ and $B = 0.20c$, hence, one third shorter, but slightly higher.

Inviscid Flow Calculation

The inviscid flow around the wing-plate junction with fairing was determined by means of the panel program KK-AERO.[39] For the computations the plate needed to be modeled as a thin flat fuselage, which was chosen to extend four chord lengths upstream of the wing and three chord lengths downstream of it and with a width of four chord lengths. The height of the wing (semispan) was taken as eight chord lengths. The relevant data that are required for the boundary-layer calculations are the streamwise velocity U_e and the lateral velocity gradient $\mathrm{d}W_e/\mathrm{d}z$ at the surface in the plane of symmetry. The output from the panel program was insufficiently smooth to serve as a direct input for the boundary-layer calculation, which is quite sensitive to irregularities in the velocity gradients when the boundary layer is close to separation. For that reason a curve fit to the panel data was used instead.

Typical results are given in Fig. 5 for the large fairing. The plotted data have been nondimensionalized with the chord length c and the freestream velocity U_∞. Furthermore, x_f is here again the distance measured along the surface, but in this case starting from the leading

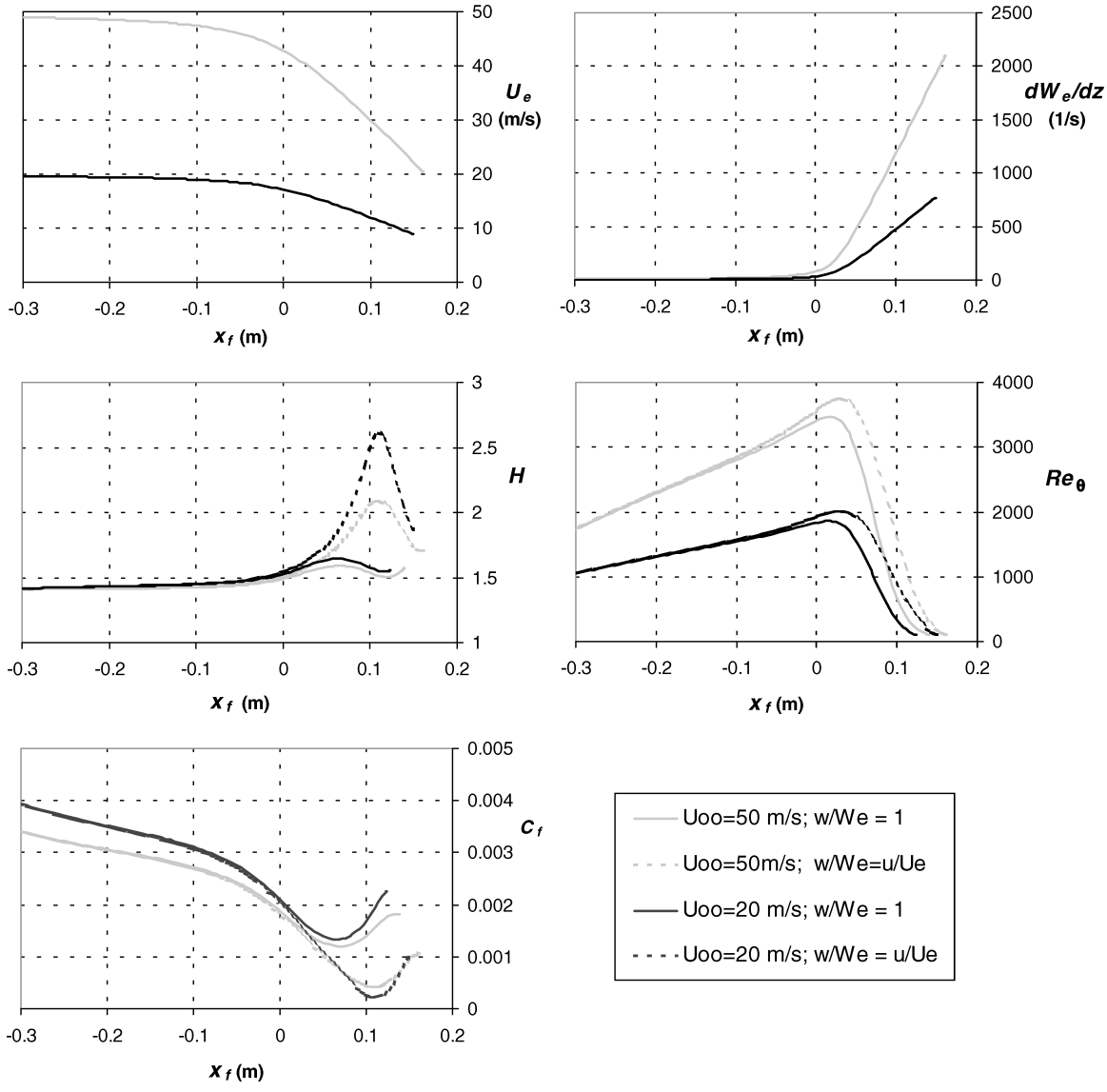

Fig. 6 Computed boundary development for the large fairing ($A = 0.21c$, $B = 0.175c$), with the effect of freestream velocity and crossflow modeling.

edge of the simulated plate. The particular fairing, hence, begins at $x_f = 3.79c$ and ends at $x_f = 4.09c$.

Boundary-Layer Calculation

The starting conditions for the boundary-layer computations were chosen such as to simulate the boundary-layer development over the sailplane fuselage upstream (Fig. 3). An initial value for the shape factor was chosen as $H = 1.4$ (a typical value for flat-plate flow). To obtain a realistic value for the initial momentum thickness, the upstream length was modeled as a 2-m-long flat plate with transition at 1.5 m. Using standard relations for the flat-plate boundary layer,[29] this yields a starting value of $\theta = 0.695$ mm at $U_\infty = 20$ m/s and $\theta = 0.439$ mm at $U_\infty = 50$ m/s. Corresponding values of Re_θ are 950 and 1500, respectively. The boundary-layer calculation is stopped when either separation is reached ($H = 3$), or when Re_θ has dropped below the laminarization threshold.

Results of the boundary calculations for the large fairing are shown in Fig. 6. Here, x_f is again the distance along the surface, but now for convenience $x_f = 0$ is set at the beginning of the fairing. The upper diagrams show the prescribed outer flow conditions, whereas the other three display some typical boundary-layer parameters. The normalized skin-friction coefficient C_f given here is defined with the constant upstream velocity U_∞ rather than the local external flow velocity U_e in order to be representative of the absolute value of the skin friction. As shown by the calculations, initially the shape factor increases, and the skin friction decreases as the boundary layer develops in an adverse pressure gradient, but on the fairing this development is reversed. Clearly, it can be seen that with the conservative crossflow assumption (14a) larger values of H are obtained, as well as a later laminarization. Also, an increase of the flow speed (Reynolds number) is seen to reduce the risk of separation, as well as delaying the laminarization.

Testing the Fairing in the Wind Tunnel

The two fairing designs were tested in the 1.80×1.25 m test section of the Subsonic Low Turbulence Tunnel of the Delft University of Technology (Fig. 7). A flat plate was installed, which spans the width of the test section. A flap at the trailing edge was used to establish a zero pressure gradient on the flat plate in the absence of the wing, which was verified by means of pressure taps in the plate.

The wing was mounted on the plate and fitted with a spanwise zigzag tape at the position of its maximum thickness in order to trip the boundary layer there and prevent separation of the laminar boundary layer. The reason for this was that the primary concern of the present investigation is the flow at the front of the wing in order to evaluate the effectiveness of the fairing. Flow separation further downstream might disturb a proper assessment of this aspect of the flow and should be eliminated in a realistic wing-body junction design by a suitable shape of the actual wing root.

First, the straight wing was tested without any fairing. Surface streamlines were visualized by applying a pigmented oil mixture on the wing and the flat plate. Tests at a freestream speed of 20 m/s display the usual picture (see Fig. 8, top) with the plate boundary layer separating in front of the wing. The S-shaped streamlines reveal that a vortex is formed, which wraps itself around the wing root.

Fig. 7 Plate-wing model in the wind tunnel.

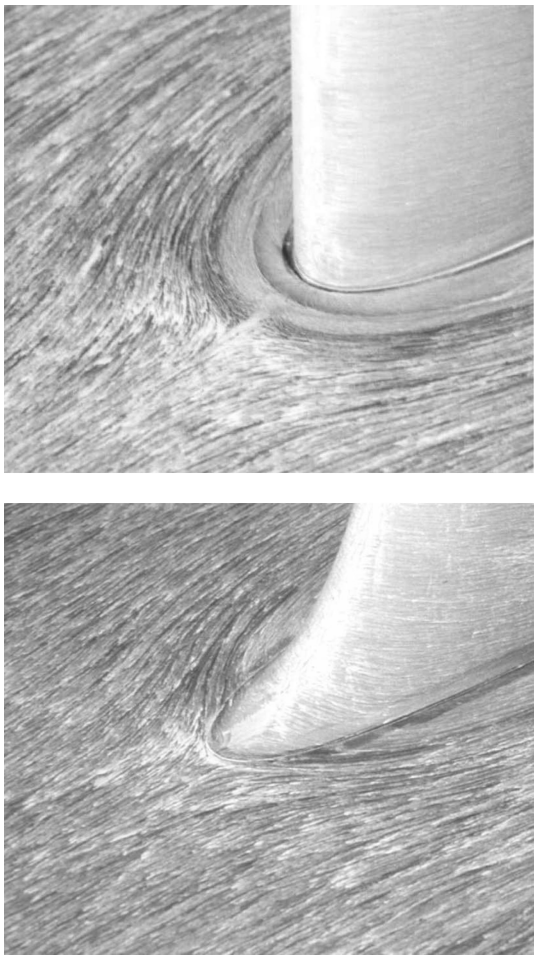

Fig. 8 Effect of the fairing on the flow near the wing-plate junction. (The second picture shows the smaller fairing.)

Next, both fairings were tested, the large fairing first. Some care was needed in visualizing the surface streamlines on the fairing, as the oil disappeared very rapidly around the wing root. Looking only at the end result of the oil pattern, this empty region might have been mistaken for a separation region. However, when the oil was applied near the wing root while the tunnel was running streamlines could indeed be seen, which moved the oil downstream in a few seconds. The cause of this is the increase in wall friction as the boundary-layer thickness decreases rapidly on the fairing; compare the results of the boundary-layer calculations (Fig. 6). As shown by the second picture of Fig. 8, streamlines can be observed all over the surface, indicating that the flow remains attached. This was verified by moving a small wool tuft just above the surface of the wing and the flat plate, which gave no evidence of any significant vortical flow near the junction.

With the smaller fairing comparable results were obtained as with the larger fairing. The streakline pattern did not display flow reversal, and the absence of separation was again confirmed with the tuft. In conclusion, it can be said that both fairing shapes satisfy in eliminating separation.

The boundary-layer calculations showed that for a given fairing geometry the maximum value of the shape factor H increases when the Reynolds number is reduced, thus bringing the flow closer to separation. Accordingly, it was tried in the tests to induce separation on the smaller fairing by lowering the tunnel speed. However, no situation was found in which the fairing lost its function and the boundary layer separated, even lowering the airspeed

that much that the oil did not flow any more, while being at its thinnest solution ($U_\infty \approx 5$ m/s). It can therefore be concluded that this fairing can be designed even more critically and that the assumption that $\tilde{w}/\tilde{W}_e = 1$ can be used with reasonable confidence to represent the flow-relieving effect in the prediction method for the boundary layer.

The fairing has to fulfill a second requirement, namely, that of promoting a quick laminarization of the flow. As the flow proceeds on the fairing, the mass flow in the boundary layer decreases rapidly, until the condition is reached where the flow fluctuations cannot maintain their strength and die out, causing the flow to become (quasi-)laminar. By using a stethoscope tube, which responds to the pressure fluctuations in the flow, regions of laminar and turbulent flow can be discerned. The observations in the experiments agreed with the predictions from the boundary-layer calculations. At an airspeed of 20 m/s, it was found that the flow on the leading edge of the fairing was turbulent up to a height of approximately 25 mm above the flat plate (which is of the order of the original boundary-layer height on the plate) and laminar above this height. As the streamlines downstream of the leading edge bend down (see Fig. 8), the upper side of turbulent wedge is at first almost horizontal. This causes this fairing to fulfill its second design requirement, in making the boundary layer on the wing laminar much closer to the root than a straight wing without fairing.

Conclusions

A design procedure for a wing-body fairing was presented, which is based on the calculation of the boundary-layer development along the attachment line of the configuration. In its present form it is applied to a symmetrical flow geometry and makes use of the corresponding simplifications. The computational effort is quite modest, which might make it a worthwhile design method, which can serve as a complementary or alternative to empirical or demanding computational-fluid-dynamics approaches.

The boundary-layer calculation was further simplified by making an additional assumption about the crossflow profile. Based on these results, two fairing geometries were realized, and wind tunnel tests revealed that both fairings worked. As the smaller fairing had been designed with some safety margin, there seems to be a further optimization possible. Further study is needed to investigate the behavior of the obtained fairing designs under off-design conditions, for example, to see whether the fairing shape remains functional under angle of attack. In addition, the performance of the fairing design in terms of overall drag reduction needs to be assessed. Other fairing geometries can be considered as well.

A logical next step in the development of the design method is to investigate to what extent a similar approach can be applied to nonsymmetrical flow situations to enable the design of a fairing for a cambered wing and/or under angle of attack.

On the part of the boundary-layer analysis, the necessity of improving the crossflow modeling can be investigated by means of checking against more accurate computations of the viscous flow or comparison with experimental data.

Further attention can be given to an improved integration of the existing design procedure, in particular streamlining the coupling between the different computational modules, which now still requires some intervention from the user, as well as a feedback of the boundary-layer results when searching for the optimum fairing shape.

References

[1]Maughmer, M., Hallman, D., Ruszkowski, R., Chappel, G., and Waitz, I., "Experimental Investigation of Wing/Fuselage Integration Geometries," *Journal of Aircraft*, Vol. 26, No. 8, 1989, pp. 705–711.

[2]Boermans, L. M. M., Nicolosi, F., and Kubrynski, K., "Aerodynamic Design of High-Performance Sailplane Wing-Fuselage Combinations," *Proceeding of the 21st International Council of the Aeronautical Sciences Conference*, ICAS 98-2.9.2, ICAS, 1998.

[3]Simpson, R. L., "Junction Flow," *Annual Review of Fluid Mechanics*, Vol. 33, 2001, pp. 415–443.

[4]Hoerner, S. F., "Interference Drag," *Fluid-Dynamic Drag*, Hoerner Fluid Dynamics, Vancouver, 1965, Chap. 8.

[5]Haines, A. B., "Aerodynamic Interference—A General Overview," *Special Course on Subsonic/Transonic Aerodynamic Interference for Aircraft*, AGARD R-712, Paper 9, AGARD, Neuilly-sur-Seine, France, 1983, Chap. 9.

[6]Simpson, R. L., "Aspects of Turbulent Boundary-Layer Separation," *Progress in Aerospace Sciences*, Vol. 32, No. 4, 1996, pp. 457–521.

[7]Arnott, A. D., "The Effect of Forward Sweep on a Wing/Body Junction Flow," Ph.D. Dissertation, Dept. of Aeronautical Engineering, Queen Mary and Westfield College, Univ. of London, 1996.

[8]Kubendran, L. R., and Harvey, W. D., "Juncture Flow Control Using Leading-Edge Fillets," AIAA Paper 85-4097, Oct. 1985.

[9]Kubendran, L. R., Bar-Sever, A., and Harvey, W. D., "Flow Control in a Wing/Fuselage-Type Juncture," AIAA Paper 88-0614, Jan. 1988.

[10]Sung, C. H., Yang, C. I., and Kubendran, L. R., "Control of Horseshoe Vortex Juncture Flow Using a Fillet," *Proceedings of the Symposium on Hydrodynamic Performance Enhancement for Marine Applications*, edited by R. H. Nadolink, Newport, RI, Oct. 1988, pp. 13–20.

[11]Pierce, F. J., Frangistas, G. A., and Nelson, D. J., "Geometry Modification Effects on a Junction Vortex Flow," *Proceedings of the Symposium on Hydrodynamic Performance Enhancement for Marine Applications Conference*, edited by R. H. Nadolink, 1988, pp. 37–44.

[12]Pierce, F. J., and Shin, J., "An Experimental Investigation of Effects of Leading-Edge Fillets on a Turbulent Junction Vortex," *Proceedings of the 2nd Symposium on Hydrodynamic Performance Enhancement for Marine Applications Conference*, edited by R. H. Nadolink, 1990, pp. 61–71.

[13]Devenport, W. J., Agarwal, N. K., Dewitz, M. B., Simpson, R. L., and Poddar, K., "Effects of a Fillet on the Flow Past a Wing-Body Junction," *AIAA Journal*, Vol. 28, No. 12, 1990, pp. 2017–2024.

[14]Devenport, W. J., Simpson, R. L., Dewitz, M. B., and Agarwal, N. K., "Effects of a Leading-Edge Fillet on the Flow Past an Appendage-Body Junction," *AIAA Journal*, Vol. 30, No. 9, 1992, pp. 2177–2183.

[15]Bernstein, L., and Hamid, S., "On the Effect of a Strake-Like Junction Fillet on the Lift and Drag of a Wing," *Aeronautical Journal*, Vol. 100, No. 992, 1996, pp. 39–52.

[16]Visbal, M. R., "Structure of Laminar Juncture Flows," *AIAA Journal*, Vol. 29, No. 8, 1991, pp. 1273–1282.

[17]Hung, C. M., Sung, C. H., and Chen, C. L., "Computation of Saddle Point of Attachment," *AIAA Journal*, Vol. 30, No. 6, 1992, pp. 1561–1569.

[18]Jupp, J. A., "Interference Effects of the A310 High-Speed Wing Configuration," *Subsonic/Transonic Configuration Aerodynamics*, Vol. AGARD-CP-285, AGARD, Neuilly-sur-Seine, France, 1980, Chap. 11.

[19]Sung, C. H., and Lin, C. W., "Numerical Investigation on the Effect of Fairing on the Vortex Flows Around Airfoil/Flat-Plate Junctures," AIAA Paper 88-0615, Jan. 1988.

[20]Devenport, W. J., and Simpson, R. L., "Flow Past a Wing-Body Junction—Experimental Evaluation of Turbulence Models," *AIAA Journal*, Vol. 30, No. 4, 1992, pp. 873–881.

[21]Green, B. E., and Whitesides, J. L., "Method for Designing Leading-Edge Fillets to Eliminate Flow Separation," *Journal of Aircraft*, Vol. 40, No. 2, 2003, pp. 282–289.

[22]Cebeci, T., and Cousteix, J., *Modeling and Computation of Boundary-Layer Flows*, Horizons/Springer-Verlag, Long Beach, Berlin, 1999, pp. 382–384.

[23]Cumpsty, N. A., and Head, M. R., "The Calculation of Three-Dimensional Turbulent Boundary Layers. Part I: Flow over the Rear of an Infinite Swept Wing," *Aeronautical Quarterly*, Vol. 18, Feb. 1967, pp. 55–84.

[24]Cumpsty, N. A., and Head, M. R., "The Calculation of Three-Dimensional Turbulent Boundary Layers. Part II: Attachment-Line Flow on an Infinite Swept Wing," *Aeronautical Quarterly*, Vol. 18, May 1967, pp. 150–164.

[25]Cumpsty, N. A., and Head, M. R., "The Calculation of Three-Dimensional Turbulent Boundary Layers. Part III: Comparison of Attachment-Line Calculations with Experiment," *Aeronautical Quarterly*, Vol. 20, May 1969, pp. 99–113.

[26]Head, M. R., "Entrainment in the Turbulent Boundary Layer," Aeronautical Research Council, R&M 3152, London, Sept. 1958.

[27]Pfenninger, W., "Laminar Flow Control—Laminarization," *Special Course on Concepts for Drag Reduction*, AGARD R-654, AGARD, Neuilly-sur-Seine, France, 1977, Chap. 3.

[28]Narasimha, R., and Sreenivasan, K. R., "Relaminarization of Fluid Flows," *Advances in Applied Mechanics*, Vol. 19, 1979, pp. 221–309.

[29]White, F. M., *Viscous Fluid Flow*, 2nd ed., McGraw–Hill, New York, 1991, pp. 450–453.

[30]Gaster, M., "On the Flow Along Swept Leading Edges," *Aeronautical Quarterly*, Vol. 18, May 1967, pp. 165–184.

[31]Poll, D. I. A., "Transition in the Infinite Swept Attachment Line Boundary Layer," *Aeronautical Quarterly*, Vol. 30, Nov. 1979, pp. 607–629.

[32]Spalart, P. R., "Direct Numerical Study of Leading-Edge Contamination," *Fluid Dynamics of Three-Dimensional Turbulent Shear Flows and Transition*, AGARD-CP-438, Paper 5, AGARD, Neuilly-sur-Seine, France, 1989, Chap. 5.

[33]Arnal, D., Juillen, J. C., Renaux, J., and Gasparian, G., "Effect of Wall Suction on Leading Edge Contamination," *Aerospace Science & Technology*, Vol. 8, No. 8, 1997, pp. 505–517.

[34]Crabtree, L. F., Kuchemann, D., and Sowerby, L., "Three-Dimensional Boundary Layers," *Laminar Boundary Layers*, edited by L. Rosenhead, Oxford Univ. Press, Oxford, 1963, pp. 409–491.

[35]Hall, P., Malik, M. R., and Poll, D. I. A., "On the Stability of an Infinite Swept Attachment-Line Boundary Layer," *Proceedings of the Royal Society, London, Series A*, Vol. 395, 1984, pp. 229–245.

[36]Pfenninger, W., "Some Results from the X-21 Program. Part I. Flow Phenomena at the Leading Edge of Swept Wings," AGARDograph 97, AGARD, Neuilly-sur-Seine, France, 1965.

[37]Preston, J. H., "The Minimum Reynolds Number for a Turbulent Boundary Layer and the Selection of Transition Device," *Journal of Fluid Mechanics*, Vol. 3, 1957, pp. 373–384.

[38]Abbott, I. H., and Von Doenhoff, A. E., *Theory of Wing Sections*, McGraw–Hill, New York, 1949, pp. 111–123.

[39]Kubrynski, K., "Design of 3-Dimensional Complex Airplane Configurations with Specified Pressure Distribution via Optimization," *Proceedings of the ICIDES III Conference*, edited by G. S. Dulikravich, 1991, pp. 263–280.